

Such an explanation of the circulatory character of particle motion in the vicinity of the cavity is qualitative in nature. A quantitative description of particle motion using the proposed model of gas distribution could be made by allowing for the rheological properties of the particles (see [7], for example).

NOTATION

a, b, initial radius and height of jet; H, R, height and width (radius) of unit; L, length of slot nozzle; p, static pressure; φ , potential of filtration velocity; U, u_0 , u_y , gas velocity, initial velocity of jet, and eddy velocity of particles; C, jet coefficient; α , drag coefficient; Q_0 , gas flow rate; d_e , equivalent diameter of particles.

LITERATURE CITED

1. M. É. Aéroov and O. M. Todes, Hydraulic and Thermal Principles of Operation of Units with Fixed and Fluidized Granular Beds [in Russian], Moscow (1968).
2. Yu. A. Buevich and G. A. Minaev, Inzh.-Fiz. Zh., 28, No. 6, 968-976 (1975).
3. Yu. A. Buevich, G. A. Minaev, and S. M. Éllengorn, Inzh.-Fiz. Zh., 30, No. 2, 197-205 (1976).
4. Yu. A. Buevich, N. A. Kolesnikova, and G. A. Minaev, Plane Problems of Gas Distribution in Granular Beds [in Russian], Moscow (1979) (Preprint/IPM AN SSSR; P129).
5. Yu. A. Buevich and G. A. Minaev, Jet Fluidization [in Russian], Moscow (1984).
6. A. D. Gosmen, V. M. Pan, A. K. Rantsel, et al., Numerical Methods of Studying Flows of a Viscous Fluid [in Russian], Moscow (1972).
7. O. V. Tyutkov and A. O. Olimpieva, Teor. Osn. Khim. Tekhnol., 10, No. 2, 248-254 (1976).

RAREFACTION WAVES IN FREE CHARGES

N. A. Azhishchev, V. A. Antipin,
A. A. Borisov, and V. A. Samoilov

UDC 534.222

It was established experimentally that the form and velocity of a rarefaction wave in free charges depends on the particle size. Three regimes of wave propagation were observed - wave, with superposed filtration, and filtration through a stationary charge.

One of the important problems in chemical engineering is intensifying heat and mass transfer in heterogeneous catalytic processes.

Significant intensification is achieved with the application of pressure pulses to the gas flow. This creates rarefaction (RW) and compression waves in the bed of dispersed material. Such a regime is realized in the periodic injection of the initial gaseous reactants into the unit and the subsequent drop in pressure [1, 2].

To develop reliable methods of designing chemical reactors operating under nonsteady conditions, it is necessary to know the mechanisms of formation and velocities of these waves and the laws governing their decay in relation to the characteristics of the dispersed medium and gas.

The goal of the present study is to experimentally investigate the velocity and structure of RW's in free charges of different dispersed materials.

It is known [3] that the rate of propagation of disturbances in disperse systems ranges from several tens to hundreds of meters a second. Thus, the base length of the measurement chamber should be several meters. The passage of an RW may be accompanied by intensive motion of particles of the dispersed material, so it is desirable to observe the displacement of the top boundary of the material.

Institute of Chemistry and Chemical Engineering, Siberian Branch, Academy of Sciences of the USSR, Krasnoyarsk. Translated from Inzhenerno-Fizicheskii Zhurnal, Vol. 52, No. 1, pp. 15-19, January, 1987. Original article submitted November 19, 1985.

TABLE 1. Physicomechanical Characteristics of the Materials

Material	Bulk density, kg/m ³	Porosity	Particle size, mm
Cement	1250	0,56	Up to 0,015
Alumina	700	0,48	0,01—0,07
Sand	1560	0,43	0,25—0,65
Fireclay	1100	0,42	0,8—1,2
Catalyst	750	0,45	2,0—2,5
Keramzit	570	0,48	9—12

In accordance with these requirements, we developed and built an experimental unit to study RW's. The unit consists of a vertical shock tube which includes a high-pressure chamber (HPC) 2.8 m long and a low-pressure chamber (LPC) 0.5 m long. Both chambers were made of glass tubing with an inside diameter of 80 mm and a wall thickness of 7 mm.

Extensometric pressure gauges were installed in the HPC at distances of 0.9, 1.6, and 2.3 m from the bottom flange. One feature of the design of the gauges was the presence of a gas buffer between the charge material and the sensitive element of the gauge.

The gauges were calibrated in accordance with the method in [4]. The transmission band of the gauges was 0-200 Hz.

The signal from the gauges was sent to a "Topaz" extensometric amplifier and then to an N-117 loop oscillograph.

The charges used consisted of the materials shown in Table 1. The height of the charge in the tests ranged from 1.6 to 2.2 m. The pressure in the HPC was a constant 0.15 MPa in all tests, while pressure in the LPC was 0.1 MPa, i.e., atmospheric.

Figure 1 shows characteristic oscillograms which were obtained. The form of the RW differs considerably from the mode of the harmonic oscillations and is obviously not determined unambiguously by the form of the sawtooth signal transmitted to the charge, as in the case in gas-liquid media [5]. The width of the signal in the gas space above the charge was $3 \cdot 10^{-3}$ sec, while the width of the RW formed in the charge was 0.1 sec.

The high-frequency pressure oscillations observed (Fig. 1a) are formed when the charge is struck by the wave packet formed by repeated reflection from the bottom of the LPC and the surface of the charge. In a charge of cement $\delta \leq 15 \mu\text{m}$, the RW is formed with a steep leading edge, and there is a distinct point at which pressure in the RW front begins to drop (Fig. 1a). In this case, the bed well transmits the high-frequency oscillations.

In the bed of alumina $\delta = 70 \mu\text{m}$ (Fig. 1b), high-frequency oscillations are absent. The RW is formed in the shape of an isosceles triangle; the amplitude of the wave does not decrease but instead remains constant over a distance of 2.4 m (the RW travels a distance 2.5 times greater than the width of the signal). Only after reflection from the bottom of the HPC does the amplitude begin to decrease (Fig. 2).

In the charge of sand $\delta = 0.2-0.6 \text{ mm}$, the point at which pressure begins to decrease becomes diffuse, and the leading edge flattens out as the RW propagates (Fig. 1c). The crest of the wave lags behind the leading edge, the leading edge and crest have different velocities. The trailing edge of the forward-traveling wave and the leading edge of the reflected wave gradually merge, and a single RW is formed from the two waves at a distance of 1.6 m.

The record on the loop oscillograph allowed us to observe not only the forward-traveling RW's, but also the reflected RW's. The latter were observed in charges with $\delta \leq 0.6 \text{ mm}$. Information on the reflected RW's was later used to determine the damping factor (Fig. 2).

The existence of two processes was detected in the bed of catalyst $\delta = 2-2.5 \text{ mm}$. "Boiling" of the charge was seen in the first stage of abrupt pressure reduction. An RW propagated in the charge in this case. The RW decayed at a distance of 0.9 m and became a purely filtration process of pressure equalization between the HPC and LPC in the stationary charge (Fig. 1d). In contrast to the charges of finely dispersed materials — where the RW plays a dominant role and filtration is absent — in the bed of catalyst $\delta = 2.0-2.5 \text{ mm}$ there was a slight rising of particles only in the top part of the charge.

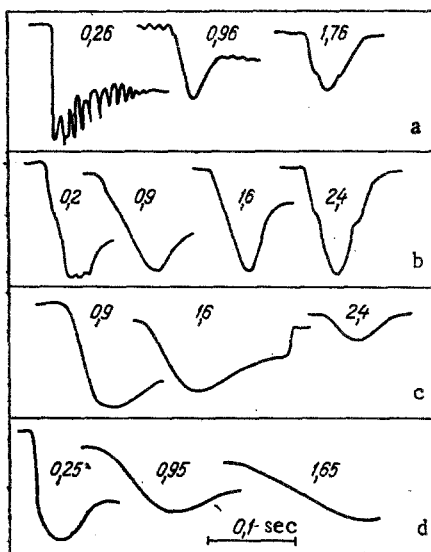


Fig. 1. Oscillograms of pressure in charges of different materials (the numbers indicate the distance in meters to the top boundary of the charge): a) cement; b) alumina; c) sand; d) catalyst.

No RW formation was observed in charges with $\delta \geq 10$ mm. Pressure equalization between the chambers occurred in less than 0.05 sec and was accompanied by the propagation of high-frequency oscillations decaying to 0 at the distance 2.4 m. Thus, RW's were completely absent in this case, the governing process was filtration, and the signal formed in the space above the charge passed through it with high-frequency components.

We used the oscillograms to calculate the velocity of the leading edge v_e and the velocity of the wave crest v_c . The first was determined as the rate at which the edge travelled between the points at which pressure began to drop, while the second was calculated from the displacement of the troughs of the waves. The results obtained are shown in Fig. 3. It can be seen from the graph that the difference in velocities increases with an increase in particle size. In charges with $\delta \leq 0.1$ mm, the velocities are equalized and the curves merge. Meanwhile, the equilibrium speed of sound $c_0 = (\gamma P / \epsilon \rho_{me})^{1/2}$ is nearly the same in these cases, i.e., an RW is present, the particles move with the gas, and filtration is absent.

In charges with $0.1 \text{ mm} \leq \delta \leq 2$ mm, v_e increases sharply from 15 to 200 m/sec, while v_c remains a constant 12 m/sec. Relative motion of the particles and gas develops, i.e., filtration occurs.

In charges with $2 \text{ mm} \leq \delta \leq 10$ mm, v_c increases from 200 to 300 m/sec and no crest is formed, i.e., no RW is observed. Here, v_c characterizes the propagation of perturbations in the gas phase in a charge with a rigid, immobile skeleton - only a filtration wave is present.

The stability of the RW can be judged from the degree of decay of the pressure amplitude (see Fig. 2). The stability of the RW increases with a decrease in the fineness of the material, although cement is an exception. This may be due to the low amplitude of the RW. A large role is played by bonding forces between particles in the cement, such forces being absent in the case of alumina [6].

Subsequent tests conducted at pressures on the order of 1 MPa showed the following qualitative changes.

In finely dispersed charges, there was no change in the structure of the leading edge of the RW and the velocity of the edge increased $v_e \sim \sqrt{P_0}$ in proportion to the initial pressure in the HPC. A series of tests conducted with ΔP between the HPC and LPC showed that the velocity of the RW is independent of the amplitude and depends only on the initial pressure in the HPC. This result is evidence of the kinematic stability of the RW, i.e., of the impossibility of the formation of shock-type pressure discontinuities. At the same time, the wave is not a simple centered RW, since there is no distinct flattening of the edge of the RW (Fig. 1a and b). Thus, the description obtained within the framework of the homogeneous

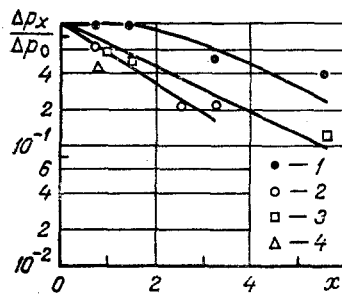


Fig. 2

Fig. 2. Dependence of the pressure on the path traveled: 1) alumina; 2) cement; 3) sand; 4) catalyst. x , m.

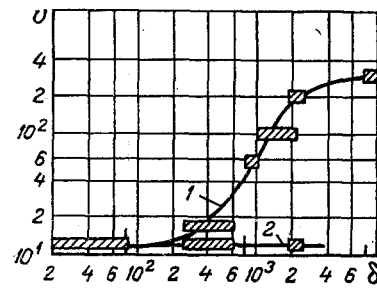


Fig. 3

Fig. 3. Velocities of the edge 1 and crest 2 in relation to the fineness of the material. The height of the rectangles corresponds to the measurement error, while the width corresponds to the particle size. v , m/sec; δ , μm .

model and its solution, analogously to gas dynamics, where the problem is easily solved in similarity coordinates of the type $\zeta = x/t$, do not produce the desired results.

In coarse materials with $\delta = 2\text{--}2.5$ mm, more significant changes occur with an increase in pressure in the HPC. The pressure at the edge changes from P_0 to P_{\min} along a line which is convex upward (the converse is true at low pressures, see Fig. 1e). The velocity of the edge becomes indeterminate, while the velocity of the crest $v_c \sim \sqrt{P_0}$ increases from 12 to 40 m/sec. Meanwhile, the velocity of the crest is nearly equal to the velocity of the RW in the finely dispersed alumina, where $v_e = 38 \pm 2$ m/sec. It can be assumed that particle mobility increases with high pressures and large pressure amplitudes at the edge, while at $P_0 \rightarrow \infty$ velocity will approach v_c and will cease to depend on particle size.

NOTATION

δ , size of particles of charge; v_e , v_c , velocity of rarefaction wave calculated for the edge and the crest, respectively; c_0 , speed of sound; γ , exponent of polytropic curve of gas; ϵ , porosity of charge; ρ_{me} , density of gas-particle mixture; ζ , similarity coordinate; x , distance; t , time; P_0 , initial pressure; P_{\min} , pressure behind the wave front.

LITERATURE CITED

1. A. Renken, M. Muller, and H. Helmrach, Chem. Ind. Techn., 47, No. 24, 1029-1032 (1975).
2. N. A. Azhishchev, V. A. Antipin, G. M. Ostrovskii, and Yu. Kh. Lokshin, "Method of impulsive fluidization of powdered materials," Inventor's Certificate No. 1036358, Byull. Izobret., No. 31 (1983).
3. V. S. Popov, Inzh.-Fiz. Zh., 14, No. 4, 716-721 (1968).
4. Kh. A. Rakhmatullin and S. S. Semenova (eds.), Shock Tubes [in Russian], Moscow (1962).
5. V. E. Nakoryakov, B. G. Pokusaev, and I. R. Shreiber, Propagation of Waves in Gas and Vapor-Liquid Media [in Russian], Novosibirsk (1983).
6. E. I. Andrianov, Methods of Determining the Structural-Mechanical Characteristics of Powdered Materials [in Russian], Moscow (1982).
7. A. N. Tikhonov and A. A. Samarskii, Equations of Mathematical Physics [in Russian], Moscow (1977).